

Experimental Quantum Error Correction

D. G. Cory,¹ M. D. Price,² W. Maas,³ E. Knill,⁴ R. Laflamme,⁴ W. H. Zurek,⁴ T. F. Havel,⁵ and S. S. Somaroo⁵

¹*Department of Nuclear Engineering, Massachusetts Institute of Technology, Cambridge, Massachusetts 02139*

²*Harvard-MIT Division of Health Sciences and Technology, Cambridge, Massachusetts 02139*

³*Bruker Instruments Inc., 19 Fortune Drive, Billerica, Massachusetts 01821*

⁴*Los Alamos National Laboratory, Los Alamos, New Mexico 87545*

⁵*BCMP, Harvard Medical School, 240 Longwood Avenue, Boston, Massachusetts 02115*

(Received 9 February 1998)

Quantum error correction is required to compensate for the fragility of the state of a quantum computer. We report the first experimental implementations of quantum error correction and confirm the expected state stabilization. A precise analysis of the decay behavior is performed in alanine and a full implementation of the error correction procedure is realized in trichloroethylene. In NMR computing, however, a net improvement in the signal to noise would require very high polarization. The experiment implemented the three-bit code for phase errors using liquid state NMR. [S0031-9007(98)06923-3]

PACS numbers: 03.67.-a, 02.70.-c, 03.65.Bz, 89.70.+c

Quantum computers exploit the superposition principle to solve some problems much more efficiently than any known algorithm for their classical counterparts. These problems include factoring large numbers [1], combinatorial searching [2], and simulations of quantum systems [3–5]. Exploiting the power of quantum computation was thought to be physically impossible due to the extreme fragility of quantum information [6,7]. This judgment seems to be overly pessimistic as quantum error-correction techniques [8–10] were found to protect quantum information against corruption. For physically reasonable models of decoherence [11] a quantum computation can be as long as desired with arbitrarily accurate answers, provided the error rate is below a threshold value [12–15]. Thus decoherence and imprecision are no longer considered insurmountable obstacles to realizing a quantum computer.

The chief remaining obstacle to quantum computing is the difficulty of finding suitable physical systems whose quantum states can be accurately controlled. Devices based on ion traps [16] have so far been limited to two bits [17]. Recently, liquid state NMR techniques have been shown to be capable of quantum computations with three bits [18,19]. Thus it is possible, for the first time, to implement the simplest quantum error-correcting codes, and so test these ideas in physical systems.

In room temperature liquid state NMR, one can coherently manipulate the internal states of the coupled spin $\frac{1}{2}$ nuclei in each of an ensemble of molecules subject to a large external magnetic field. Although the set of accessible states is highly mixed, it has been shown that experimental methods exist that can be used to isolate the pure state behavior of the system, thus permitting limited application of NMR to quantum computation [20,21]. A detailed description of these methods can be found in [11]. Here we describe the implementation of a quantum error-correcting code which compensates for small phase errors. The behavior of this code was measured for two systems: The ^{13}C labeled carbons in alanine sub-

ject to the correlated phase errors induced by diffusion in a pulsed magnetic field gradient, and the proton and two labeled carbons in trichloroethylene (TCE) subject to its natural relaxation processes. In alanine, we observed correction of first-order errors using a precise analysis of the decay behavior of a given input state. The full error-correction procedure (including the final Toffoli gate) was implemented in TCE to demonstrate the expected state preservation of an arbitrary coherent input.

Although our experiments validate the usefulness of error correction for quantum computing with pure states, there is a substantial loss of signal associated with the use of ancilla spins in weakly polarized systems. We argue that in this setting, the loss of signal involved in exploiting ancillas removes any advantage for computation gained by error correction, at least unless the system is sufficiently polarized to enable the generation of nearly pure states. Nevertheless, our experiments demonstrate that error-correcting codes can be implemented, and that they behave as predicted.

The simple three-bit quantum error-correcting code used here is designed to compensate to first order for small random phase fluctuations. These fluctuations constitute a random evolution of the state

$$\begin{aligned} |b_1 b_2 b_3\rangle &\rightarrow e^{-i(\theta_1 \sigma_z^1 + \theta_2 \sigma_z^2 + \theta_3 \sigma_z^3)} |b_1 b_2 b_3\rangle \\ &= e^{i[(-1)^{b_1} \theta_1 + (-1)^{b_2} \theta_2 + (-1)^{b_3} \theta_3]} |b_1 b_2 b_3\rangle, \end{aligned} \quad (1)$$

where b_i is 0 or 1, θ_i is a random phase variable, and σ_z^i is the Pauli matrix acting on the i th spin. The θ_i depend on the error rates in the model, which is described in detail below.

The error-correcting code is a phase variant of the classical three-bit majority code with a decoding technique that preserves the quantum information in the encoded state [9]. Let $|\pm\rangle = (|0\rangle \pm |1\rangle)/\sqrt{2}$. The state $(\alpha|000\rangle + \beta|100\rangle)$ is encoded as $\alpha|+++ \rangle + \beta|--- \rangle$ by a unitary transformation. The first-order expansion of the operator in Eq. (1) in the small random phases is

$$\mathbf{1} - i\theta_1\sigma_z^1 - i\theta_2\sigma_z^2 - i\theta_3\sigma_z^3, \quad (2)$$

which evolves the encoded state to

$$\begin{aligned} \alpha|+++ \rangle + \beta|--- \rangle \rightarrow & \alpha|+++ \rangle + \beta|--- \rangle - i\theta_1(\alpha|--+ \rangle + \beta|+- \rangle) - i\theta_2(\alpha|+- \rangle + \beta|--+ \rangle) \\ & - i\theta_3(\alpha|++- \rangle + \beta|--+ \rangle). \end{aligned} \quad (3)$$

The different errors map the encoded state into orthogonal subspaces. By measuring the two observables $\sigma_z^1\sigma_z^3$ and $\sigma_z^2\sigma_z^3$ the subspace can be identified. Thus one can determine which error occurred without destroying the encoded quantum information. After decoding, the original state of the first spin can then be restored by a unitary transformation, while the other two spins contain information (the syndrome) about the error which occurred. A network which accomplishes the encoding, decoding, and error-correction steps is shown in Fig. 1.

In NMR experiments, nonunitary processes are classified as spin-lattice and spin-spin relaxation [22,23]. For spin $\frac{1}{2}$ nuclei, both processes are due to fluctuating local magnetic fields. The three spin code corrects for errors due to locally fluctuating fields along the z axis.

We focus on a weakly coupled three-spin system where the strongest contribution to coherence loss is from external fields which contribute the Hamiltonian

$$\mathcal{H}_R \equiv \gamma^1 \mathbf{I}^1 \cdot \mathbf{B}^1(t) + \gamma^2 \mathbf{I}^2 \cdot \mathbf{B}^2(t) + \gamma^3 \mathbf{I}^3 \cdot \mathbf{B}^3(t), \quad (4)$$

where $\mathbf{I} = (\mathbf{I}_x, \mathbf{I}_y, \mathbf{I}_z)$ and $\mathbf{I}_u = \frac{1}{2}\sigma_u$ ($u = x, y, z$). The x and y components of the external fields do not contribute significantly to loss of coherence in our experiments. The induced random phase fluctuations are identical to those described in Eq. (1). As a result, the off-diagonal elements of the density matrix decay exponentially at a rate which depends on the fields \mathbf{B}^k at each spin, their gyromagnetic ratios γ^k , the coherence order, and the zero frequency components of the spectral densities of the fields. The ‘‘coherence order’’ is the difference between the total angular momenta along the z axis of the two states $|b\rangle, |b'\rangle$ (in units of $\hbar/2$) which define a matrix element $|b'\rangle\langle b|$ [24].

To obtain a clean demonstration of error correction, a simple error model was implemented precisely in the case of alanine. This implementation used the random molecular motion induced by diffusion in a constant field gradient to mimic the effect of a slowly varying

random field. This is achieved by turning on an external field gradient $\nabla_z \mathbf{B} = \partial B_z / \partial z$ across the sample for a time δ . This modifies the magnetization in the sample with a phase varying linearly along the z direction according to $\partial \phi / \partial z = n \delta \gamma \partial B_z / \partial z$, where n is the coherence order of the density matrix element and γ is the gyromagnetic ratio. A reverse gradient is used to refocus the magnetization after allowing molecular diffusion to take place for the amount of time t . As a result of random spin displacement Δz , the phases of the spins are not returned to their original values but are randomly modified by $(n \delta \gamma \partial B_z / \partial z) \Delta z$. For a Gaussian displacement profile with a width of $\sqrt{2Dt}$, the effective decoherence time of this process is proportional to the diffusion constant D as well as to the square of the coherence order n [24]:

$$\frac{1}{\tau} = \left(\frac{\partial \phi}{\partial z} \right)^2 D = \gamma^2 (\nabla_z \mathbf{B})^2 n^2 \delta^2 D. \quad (5)$$

This artificially induced ‘‘decoherence’’ in the alanine experiments is an example of completely correlated phase scrambling. This occurs naturally if all the spins have equal gyromagnetic ratios in the slow motion regime. We used TCE to demonstrate error correction in the presence of the natural decoherence.

Most NMR experiments are described using the product operator formalism [25]. This formalism describes the state as a sum of products of the operators $\mathbf{I}_x^k, \mathbf{I}_y^k, \mathbf{I}_z^k$. The identity component of such a sum is the same for any state and is usually suppressed to yield the ‘‘deviation’’ (traceless) density matrix. The effect of error correction can be understood from the point of view of this formalism. As an example, consider encoding the state \mathbf{I}_z^1 using two ancillas initially in their ground states. The initial state is described by

$$\rho_A = \mathbf{I}_z^1 (\frac{1}{2}\mathbf{1} + \mathbf{I}_z^2) (\frac{1}{2}\mathbf{1} + \mathbf{I}_z^3). \quad (6)$$

After encoding the state is

$$\rho_B \equiv \frac{1}{4} (\mathbf{I}_x^1 + \mathbf{I}_x^2 + \mathbf{I}_x^3 + 4 \mathbf{I}_x^1 \mathbf{I}_x^2 \mathbf{I}_x^3). \quad (7)$$

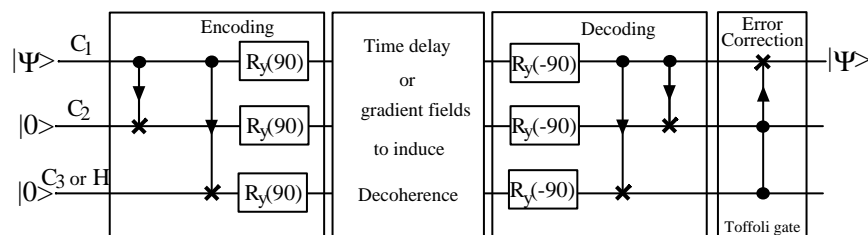


FIG. 1. Network for encoding, decoding, and error correction. The circuit describes the evolution of the three bits as a function of time. The gate $\bullet \rightarrow \times$ corresponds to a control-not. $R_y(90)$ represent a rotation by an angle of $\pi/2$ around the y axis of a single bit. The Toffoli gate flips the target bit (\times) if the two control bits (\bullet) are in the state $|1\rangle$. A detailed implementation of these gates is given in [18]. The information carrying bit is carbon 1 (see Figs. 2 and 3) in both experiments.

In the case of completely correlated phase errors, this decays as

$$\begin{aligned} \rho_C \equiv & \frac{1}{4} [(\mathbf{I}_x^1 + \mathbf{I}_x^2 + \mathbf{I}_x^3)e^{-t/\tau} \\ & + (3\mathbf{I}_x^1\mathbf{I}_x^2\mathbf{I}_x^3 + \mathbf{I}_x^1\mathbf{I}_y^2\mathbf{I}_y^3 + \mathbf{I}_y^1\mathbf{I}_x^2\mathbf{I}_y^3 + \mathbf{I}_y^1\mathbf{I}_y^2\mathbf{I}_x^3)e^{-t/\tau} \\ & + (\mathbf{I}_x^1\mathbf{I}_x^2\mathbf{I}_x^3 - \mathbf{I}_x^1\mathbf{I}_y^2\mathbf{I}_y^3 - \mathbf{I}_y^1\mathbf{I}_x^2\mathbf{I}_y^3 - \mathbf{I}_y^1\mathbf{I}_y^2\mathbf{I}_x^3)e^{-9t/\tau}]. \end{aligned} \quad (8)$$

Decoding and error correction mixes these states together so as to cancel the initial decay of the first spin,

$$\rho_E^1 \equiv \frac{1}{8} \mathbf{I}_z^1 (9e^{-t/\tau} - e^{-9t/\tau}) \approx \mathbf{I}_z^1 (1 - \frac{9}{2} t^2/\tau^2 + \dots). \quad (9)$$

The effect of error correction can be seen from the absence of terms depending linearly on t .

In the alanine experiments, each of the four product operators in the sum of Eq. (6) was realized in a separate experiment, and the final state after encoding and decoding inferred by adding the results. The loss of polarization over time in each product operator was measured explicitly in each experiment. The results were added computationally to simulate the effect of the Toffoli gate and are shown in Fig. 2. This method has the advantage of permitting a detailed analysis of the relevant relaxation pathways. The initial slopes of the decay curves for each operator were estimated and added as required for error correction. The resulting slope is zero within experimental errors. Thus the net curve has quadratic behavior for small delays.

The goal of our experiments with TCE was to establish the behavior of encoding followed by decoding and

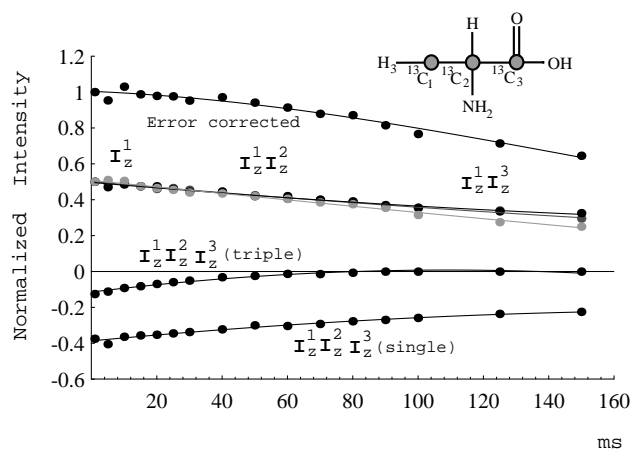


FIG. 2. The intensities of the magnetization of the first spin after applying the dephasing and decoding procedures described in the text, together with single exponential fits to the intensities versus the dephasing time τ . The relevant coupling frequencies are 53.9 and 34.8 Hz between adjacent carbons. The three mixed states \mathbf{I}_z^1 , $\mathbf{I}_z^1\mathbf{I}_z^2$, $\mathbf{I}_z^1\mathbf{I}_z^3$, evolved as single quantum coherences during τ , whereas $\mathbf{I}_z^1\mathbf{I}_z^2\mathbf{I}_z^3$ evolved as a mixture of single and triple quantum coherences, which have been plotted separately (single and triple). Their sum (error corrected) give the intensities the same experiment using a pseudopure state (see text). The initial slope of the sum is close to zero, thus showing that the error-correction procedure was able to cancel dephasing to first order.

error correction on all possible initial states subject to the natural decoherence and dephasing. The spins were prepared in the states

$$\rho(\frac{1}{2}\mathbf{1} + \mathbf{I}_z^2)(\frac{1}{2}\mathbf{1} + \mathbf{I}_z^3), \quad (10)$$

with ρ one of the four inputs $\frac{1}{2}\mathbf{1}$, \mathbf{I}_z^1 , \mathbf{I}_x^1 , \mathbf{I}_y^1 . Any possible input is just a linear combination of these four states. We used gradient methods to directly generate the four states of Eq. (10). They were then subjected to pulse sequences for encoding, decoherence, and decoding (experiment I). The reduced density matrix on the first spin (the output) was measured. In the second experiment (II) decoding was followed by error correction (i.e., physical implementation of the Toffoli gate so that the whole circuit of Fig. 1 was implemented) before the output was determined. Decoherence was implemented in two ways. The first involved a variable delay during which natural dephasing takes place. In the second implementation, we inserted pulses for each possible phase error (sign flips on at most one spin). Pulse sequences can be found in [26]. Ideally the output would be identical to the input. The measured outputs were compared to the ideal ones by computing the “entanglement fidelity” [27]. This is a useful measure of how well the quantum information in the input is preserved. Entanglement fidelity is the sum of the correct polarization left in the output state for each input. More precisely, given input \mathbf{I}_a^1 , let f_a be the relative polarization of \mathbf{I}_a^1 in the output compared to the input. Then $f = \frac{1}{4}(1 + f_x + f_y + f_z)$, and this formula is correct for processes which do not affect the completely mixed state $\frac{1}{2}\mathbf{1}$. The results for nine different delays are shown in Fig. 3. The curves show that error correction decreases the initial slope by a factor of ~ 10 (by square fit to the logarithm).

Our demonstration of error correction does not imply that error correction can be used to overcome the problems of high temperature ensemble quantum computing. In this model of quantum computing, the initial state can be described as a small, linear deviation from the infinite temperature equilibrium. Thus, the deviation is proportional to a Hamiltonian of n weakly interacting particles. In this limit no method of error correction based on externally applied, time dependent fields can improve the polarization of any particle by more than a factor proportional to \sqrt{n} [28]. If one wishes to use error correction an even bigger problem is encountered: The initial state of the ancillas used for each encoding/decoding cycle must be pure. In the high temperature regime, the best we can do is to generate a pseudo pure deviation in the ancillas. Unfortunately, this deviation has to be created *simultaneously* on all ancillas, leading to an exponential reduction in polarization as a function of the total number of ancillas required [29]. This reduction in polarization is not recoverable by error correction. In fact, further analysis shows that an initial polarization of order unity is required for error correction to yield a net gain. Another

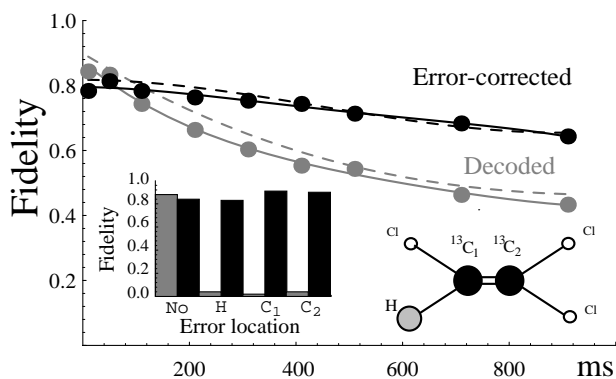


FIG. 3. Experimentally determined entanglement fidelities for the TCE experiments after decoding (gray) and after decoding and error correction (black). The relevant coupling frequencies are 200.7 Hz between H and C1, and 103.1 Hz between C1 and C2. The pulse sequences for encoding, decoding, and error correction take about 35 ms. In this experiment the Toffoli gate was realized by a set of pulses. The histogram represent the fidelities when a single sign flip error has been induced on H, C1, or C2 clearly exhibiting the improvement from error correction. The graph shows continuous curves interpolating the data points. The broken curves were determined by simulating the pulse sequence using the measured coupling constants and estimated T_2 's of 1.1 s (C1), 0.6 s (C2) and 3 s (H). Differences between experimental and theoretical curves are attributed to lack of precise knowledge of the error model. Errors in the data points are approximately 0.05. Note that since the proton T_2 is much longer than that of the carbons, the long term gain in fidelity is partially due to recovery of polarization from the proton. The demonstration of error correction lies in the initial slope. The curves show that error correction decreases the initial slope by a factor of ~ 10 (by least squares fit to the logarithm).

problem is the inability to reuse ancilla bits. This has two consequences. The first is that decoherence rapidly removes information in the state, leading to computations which are logarithmically bounded in time [30]. Second, the total number of ancillas required is proportional to the time-space product of the computation, rather than to a power of its logarithm.

Our work shows that liquid state NMR can be used to test fundamental ideas in quantum computing. Our experiments demonstrate for the first time the state preserving effect of the three-bit phase error-correcting code. The first-order behavior was established to high accuracy for a specific state in alanine, while the overall effect was observed and the improvement in state recovery verified in TCE. These experiments confirm not only the validity of theories of quantum error correction in a simple case, but also demonstrate the ability, in liquid state NMR, to control the state of three spin-half particles. This is an important advance for quantum computing, as this is the first system where this degree of control has been successfully implemented.

We thank Jeff Gore for his help with the simulations. This work was supported by the U.S. Army Research Office, DARPA, and the National Security Agency.

- [1] P. W. Shor, in *Proceedings of the 35th Annual Symposium on Foundations of Computer Science* (IEEE Press, Los Alamitos, CA, 1994), pp. 124–134.
- [2] L. K. Grover, quant-ph/9605043.
- [3] R. P. Feynman, *Found. Phys.* **16**, 507–531 (1986).
- [4] S. Lloyd, *Science* **273**, 1073–1078 (1996).
- [5] C. Zalka, *Proc. R. Soc. London A* **454**, 313–322 (1998).
- [6] R. Landauer, *Philos. Trans. R. Soc. London* **353**, 367–376 (1995).
- [7] W. G. Unruh, *Phys. Rev. A* **51**, 992–997 (1995).
- [8] P. W. Shor, *Phys. Rev. A* **52**, 2493 (1995).
- [9] A. Steane, *Proc. R. Soc. London A* **452**, 2551 (1996).
- [10] P. W. Shor, *SIAM J. Comput.* **26**, 1484 (1997).
- [11] E. Knill, I. Chuang, and R. Laflamme, *Phys. Rev. A* **57**, 3348–3363 (1998).
- [12] E. Knill, R. Laflamme, and W. H. Zurek, *Science* **279**, 342 (1998).
- [13] D. Aharonov and M. Ben-Or, in *Proceedings of the 29th Annual ACM Symposium on the Theory of Computing* (ACM Press, New York, 1996), pp. 176–188; quant-ph/9611025.
- [14] J. Preskill, *Proc. R. Soc. London A* **454**, 385–410 (1998).
- [15] A. Yu. Kitaev, *Usp. Mat. Nauk* **52**, 53–112 (1997).
- [16] J. Cirac and P. Zoller, *Phys. Rev. Lett.* **74**, 4091 (1995).
- [17] C. Monroe, D. M. Meekhof, B. E. King, W. M. Itano, and D. J. Wineland, *Phys. Rev. Lett.* **75**, 4714 (1995).
- [18] D. G. Cory, M. P. Price, and T. F. Havel, *Physica (Amsterdam)* **120D**, 82–101 (1998).
- [19] R. Laflamme, E. Knill, W. H. Zurek, P. Catasti, and S. V. S. Mariappan, *Proc. Trans. R. Soc. London A* **356**, 1941–1948 (1998).
- [20] D. G. Cory, A. F. Fahmy, and T. F. Havel, *Proc. Natl. Acad. Sci. U.S.A.* **94**, 1634–1639 (1997).
- [21] N. A. Gershenfeld and I. L. Chuang, *Science* **275**, 350–356 (1997).
- [22] A. Abragam, *Principles of Nuclear Magnetism* (Clarendon Press, Oxford, UK, 1961).
- [23] R. R. Ernst, G. Bodenhausen, and A. Wokaun, *Principles of Nuclear Magnetic Resonance in One and Two Dimensions* (Clarendon Press, Oxford, UK, 1987).
- [24] C. P. Slichter, *Principles of Magnetic Resonance* (Springer-Verlag, Berlin, 1990), 3rd ed.
- [25] O. W. Sørensen, G. W. Eich, M. H. Levitt, G. Bodenhausen, and R. R. Ernst, *Prog. Nucl. Magn. Reson. Spectrosc.* **16**, 163 (1983).
- [26] For a pulse sequence of this experiment see <http://www.c3.lanl.gov/~knill/trnsp.html>
- [27] B. Schumacher, *Phys. Rev. A* **54**, 2614–2628 (1996).
- [28] O. W. Sørensen, *Prog. Nucl. Magn. Reson. Spectrosc.* **21**, 503–569 (1989).
- [29] W. S. Warren, *Science* **277**, 1688–1698 (1997).
- [30] D. Aharonov and M. Ben-Or, quant-ph/9611028, 1996.